Aerosol and Air Quality Research, 17: 2328–2337, 2017

ISSN: 1680-8584 print / 2071-1409 online
doi: 10.4209/aaqr.2017.07.0229

Characterization and SCR Performance of Nano-Structured Iron-Manganese Oxides: Effect of Annealing Temperature

Qian Li[1], Haibo Liu[1*], Tianhu Chen[1], Dong Chen[1], Changai Zhang[1], Bin Xu[1], Chengzhu Zhu[1], Yang Jiang[2]**

[1] *Laboratory for Nanomineral and Environmental Material, School of Resources and Environmental Engineering, Hefei University of Technology, Hefei, Anhui 230009, China*
[2] *School of Materials Science and Engineering, Hefei University of Technology, Hefei, Anhui 230009, China*

ABSTRACT

Nano-structured iron-manganese oxides composite was prepared by annealing of natural Mn-rich limonite at different temperatures (500, 600, 700, 800°C). Their SCR performances of NO removal by NH_3 were evaluated, and SEM, TEM, XRD, XRF, BET, XPS, Raman, NH_3-TPD were utilized to analyze the catalytic mechanism. The results indicated that after annealing at 500°C, the as-prepared iron-manganese oxides exhibited the best SCR performance in NO conversion and N_2 selectivity (over 80%) at the temperature window of 150–300°C. An increase in annealing temperature from 500 to 800°C significantly increased the particle size resulting in the decrease of surface areas, active sites, and then SCR performances. The experimental results suggested the natural Mn-rich limonite was an excellent precursor for preparing iron-manganese oxides and possessed excellent SCR performance of NO removal by NH_3. This study will provide a novel way for the preparation of SCR catalyst and exploit a new application field for natural limonite.

Keywords: Natural limonite; Iron-manganese oxides; Selective catalytic reduction; NO conversion; N_2 selectivity.

INTRODUCTION

Nitric oxides originating from stationary power plants are important pollutants causing a series of serious environmental problems, such as acid rain, ozone depletion, photochemical smog and greenhouse gas (Sahu, 2015; Zahaf, 2015; Lu *et al.*, 2016; Rattigan *et al.*, 2016). Selective catalytic reduction (SCR) has been proved to be an effective technology for the reduction of NO_x by NH_3 over different catalysts due to its high efficiency and economic efficiency (Yu, 2015; Jiang *et al.*, 2017; Yu *et al.*, 2017). Among these catalysts, V_2O_5/TiO_2 in combination with MoO_3 and WO_3 has been commercialized in consequence of its high catalytic reactivity, including NO conversion, N_2 selectivity and resistance to sulfur poisoning, and mechanical strength. In view of high reaction temperature and environmental toxicity of vanadium species (Liu and He, 2010; Liu *et al.*, 2011b; Ma *et al.*, 2011; Youn *et al.*, 2016), vanadium-free catalysts attracted much attention including M-zeolite catalysts (M-Fe, Cu, Mn, Mo) (Pérez-RamíRez *et al.*, 2004; Yoshida *et al.*, 2004; Liu *et al.*, 2011a; Ochońska *et al.*, 2012; Schuricht and Reschetilowski, 2012; Mejri *et al.*, 2016) and metal oxides catalysts (Fe, Mn, Cu, Ce, Cr, etc.) (Kato *et al.*, 1981; Baksh *et al.*, 1992; Kapteijn *et al.*, 1994; Chen *et al.*, 1995; Schneider *et al.*, 1995; Zhu *et al.*, 1999; Eigenmann *et al.*, 2006; Min *et al.*, 2007; Xu *et al.*, 2008; Liu *et al.*, 2010; Liu *et al.*, 2013a; Shin *et al.*, 2016).

Besides the high NO conversion and N_2 selectivity, iron oxides and manganese oxides are significantly favorable catalysts among the vanadium-free catalysts due to low cost and high low-temperature activity, respectively. In the previous reports, iron oxide catalysts mostly contained α-Fe_2O_3 (Liu *et al.*, 2017), γ-Fe_2O_3 (Yang *et al.*, 2013; Huang *et al.*, 2014) and rod-shaped Fe_2O_3 (Mou *et al.*, 2012). The results indicated that iron oxides catalyst exhibited an excellent SCR performance at a temperature range of 200-400°C. Mou *et al.* (2012) reported that rod-shaped α-Fe_2O_3 kept a NO conversion of over 80% at the window ranged from 200 to 400°C, and confirmed γ-Fe_2O_3 had better SCR activity than α-Fe_2O_3. Afterwards, Liu *et al.* (2013a) also verified both α-Fe_2O_3 and γ-Fe_2O_3 exhibited remarkably different NO conversion. The latter was better due to the presence of higher oxygen defect and the formation of few stable nitrates in the reaction process. Compared with iron oxides, manganese oxides are generally used as active

* Corresponding author.
Tel.: +86 15856995526
E-mail address: liuhaibosky116@hfut.edu.cn
** Corresponding author.
Tel.: +86 13956099615; +86 0551-62903990
E-mail address: chentianhu@hfut.edu.cn

composition supported on a carrier. The spent carrier materials included TiO_2 (Fang *et al.*, 2014; Putluru *et al.*, 2015), spinel (Yang *et al.*, 2011; Yang *et al.*, 2016), zeolite (Kim *et al.*, 2012; Huang *et al.*, 2016), and so forth. These results indicated that manganese oxides showed a remarkable activity for SCR at the temperature range between 100 to 300°C. Putluru *et al.* (2015) demonstrated that 25 wt% Mn0.75Fe0.25Ti-DP catalyst prepared by deposition precipitation exhibited superior low-temperature SCR, and it was probably due to the presence of amorphous phases of manganese oxides and iron oxides with the properties of high surface area, high total acidity, acid strength and so on.

On the other hand, according to the previous report (Liu *et al.*, 2013d), natural limonite widely spread on the earth and the crystal iron is usually substituted by aluminum, manganese, zinc, etc. It is normal for the coexistence of iron and manganese in limonite, and the amount of manganese depends on the genesis of limonite. In addition, natural limonite is a the eco-friendly, low-cost mineral material. According to the decomposition characteristic of limonite as the previously reported (Liu *et al.*, 2013c), it was speculated that iron and manganese oxides with nano-porous structure and high surface area could be obtained by the thermal decomposition of limonite. Meanwhile, the iron and manganese oxides are believed to be of great potential in SCR of NO by NH_3. Therefore, in this present study, natural Mn-rich limonite was used to prepare iron and manganese oxides for SCR catalysts. The effect of preparation temperature on the structure and SCR activity of the catalysts was investigated using the laboratory-scale catalytic system and characterization of XRD, N_2 adsorption-desorption, XPS, SEM, TEM, Raman and NH_3-TPD. The objectives are to prepare a eco-friendly, low-cost and high-effective SCR catalyst by the thermal decomposition of natural limonite, and to build the relationship between preparation temperature, pore texture and SCR activity of iron and manganese oxides catalysts.

EXPERIMENTAL

Catalyst Preparation

The iron and manganese oxides (IMO) catalysts were prepared by annealing of limonite in air for 1 h at different temperatures (500, 600, 700, 800°C). Thermal treatment was carried out in a tube furnace with a programmable temperature controller. After annealing, catalysts were cooled down to room temperature and then sieved to 30–60 mesh (0.25–0.55 mm) for further characterization and activity evaluation. To simplify the sample labeling, LT (T = 500, 600, 700, 800) used to denote the catalyst was prepared from the annealing of limonite at T °C.

Catalytic Activity Testing

The testing of SCR performance of the as-prepared catalysts was carried out in a fixed-bed quartz tube reactor with an inner size of 6 mm and 0.25 g of catalyst was used each time. The simulated flue gases were composed of 1000 ppm of NH_3, 1000 ppm of NO, 3% of O_2, and balanced with Ar, and a gas flow rate of 300 mL min^{-1} was controlled by mass flow controllers (Sevenstar D08, Beijing). The catalytic activity testing was conducted in a temperature range of 100–450°C with a gas hourly space velocity (GHSV) of 72,000 h^{-1}. The temperature was regulated through a programmable temperature controller. The concentrations of NO, NO_2, NH_3, and N_2O were monitored by a Fournier transform IR (FT-IR) spectrometer. The schematic diagram of the experimental set-up is displayed in Fig. 1.

As the SCR reaction reached a steady state, the gases concentration was recorded and then NO conversion and N_2 selectivity were calculated in terms of the following equations:

$$\text{NO conversion} = \frac{[NO]_{in} - [NO]_{out}}{[NO]_{in}} \times 100\% \quad (1)$$

$$N_2 \text{ selectivity} = \frac{[NO_x]_{in} + [NH_3]_{in} - [NO_x]_{out} - [NH_3]_{out} - 2\times[N_2O]_{out}}{[NH_3]_{in} - [NH_3]_{out} + [NO_x]_{in} - [NO_x]_{out}} \times 100\% \quad (2)$$

$$[NO_x] = [NO] + [NO_2] \quad (3)$$

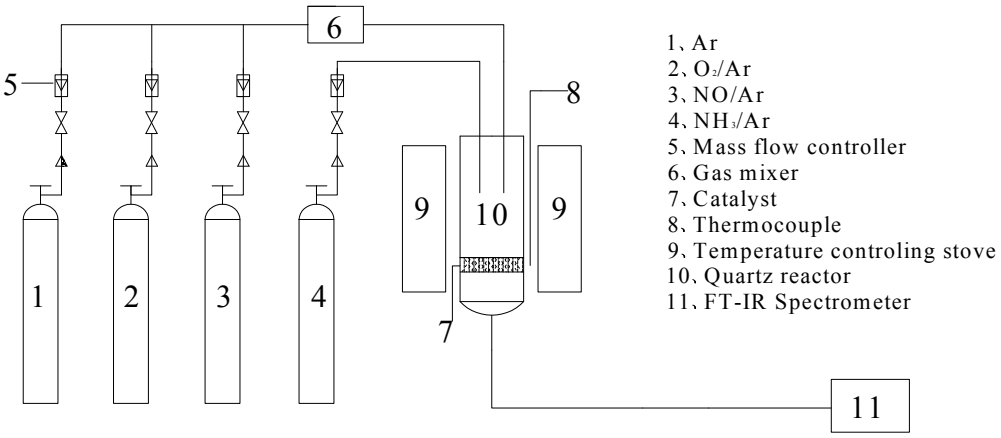

Fig. 1. Schematic diagram of SCR of NO by NH_3 over catalysts.

Catalyst Characterization

Crystal phases of samples were determined using an X-ray diffractometer (XRD, Dandong DS-2700) with 2θ ranged between 15° and 70° and a step size of 4° min^{-1} operated at 50 KV and 100 mA using Cu Kα radiation.

The specific surface area, pore volume and pore size distribution were measured based on N_2 adsorption-desorption at liquid nitrogen temperature with a Quantachrome (NOVA3000e) analyzer. The samples were degassed at 110°C for 24 h before analysis.

A scanning electron microscope (SEM, SU8020) and a transmission electron microscope (HRTEM, JEM-2100) were used to characterize the morphology of the samples.

An X-ray photoelectron spectroscopy (ESCALAB250Xi) was used to determine the Fe2p and Mn2p binding energies with Al Kα radiation. The binding energies were referenced to the C 1 s line at 284.7 eV.

Temperature-programmed desorption of NH_3 (NH_3-TPD) experiments were used to characterize the surface acid of the prepared catalysts. NH_3-TPD was carried out in a temperature of 50–500°C in a micro-reactor. The temperature was measured using a K-type thermocouple. Molecules from the outlet of the micro-reactor were monitored using a quadrupole mass spectrometer (Hiden QIC-20). Before desorption, the sample was saturated by NH_3 judging by $^{15}NH_3$ signal at the temperature of 50°C. Afterwards, desorption was performed with a rate of 10 °C min^{-1} from 50 to 500°C.

Raman spectra of samples were carried out at room temperature using a confocal Raman spectrometer (LabRAM HR Evolution). Raman signal was excited using the 532 nm wavelength of an argon ion laser source. Typical acquisition time was 10 s and the wavenumber region was 100–1000 cm^{-1} with a spectral resolution of 1 cm^{-1}.

RESULTS AND DISCUSSION

SCR Performance

The SCR performances of nano-sized iron-manganese oxides catalysts as a function of temperature from 100 to 450°C are shown in Fig. 2. The reaction temperature considerably influenced the NO conversion. In particular, the NO conversion increased firstly and then decreased with an increase of reaction temperature. The increasing reaction temperature favored the SCR reaction up to 300°C consequently resulting in the increase of NO conversion. The decrease of NO conversion is attributed to the oxidation of NH_3 at the temperature over 300°C, which can be deduced from the increase of NH_3 conversion as seen in Fig. 2. On the other hand, L500 exhibited a high NO conversion over 80% at the temperature window of 150–300°C, while L600 only had a NO conversion over 80% at 250°C. Meanwhile, the L700 and L800 presented a relatively low NO conversion (lower than 60%). Meanwhile, the N_2 selectivity of these samples as a function of temperature is also displayed in Fig. 3. It is not hard to find an increase of reaction temperature gradually decreased the N_2 selectivity, and an increase of annealing temperature slightly increased the N_2 selectivity. Even so, the N_2 selectivity was still more than 80% when the reaction temperature was not more than

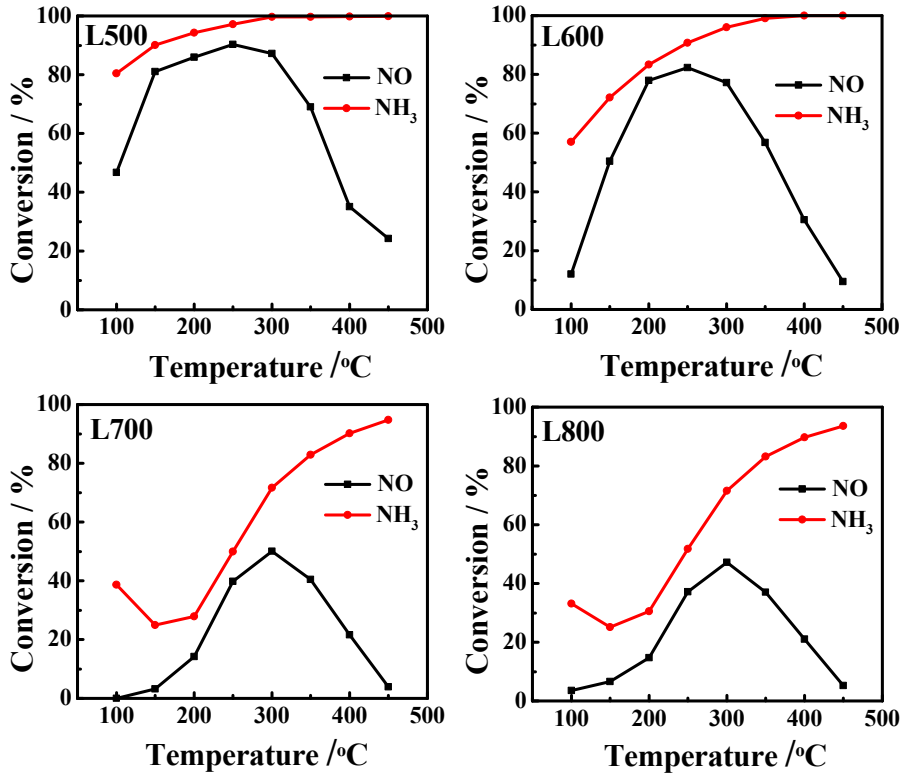

Fig. 2. The NO and NH_3 conversion of different iron-manganese oxides catalysts (Reaction condition: NO = 1000 ppm, NH_3 = 1000 ppm, O_2 = 3 vol%, and balance of Ar, GHSV = 72,000 h^{-1}).

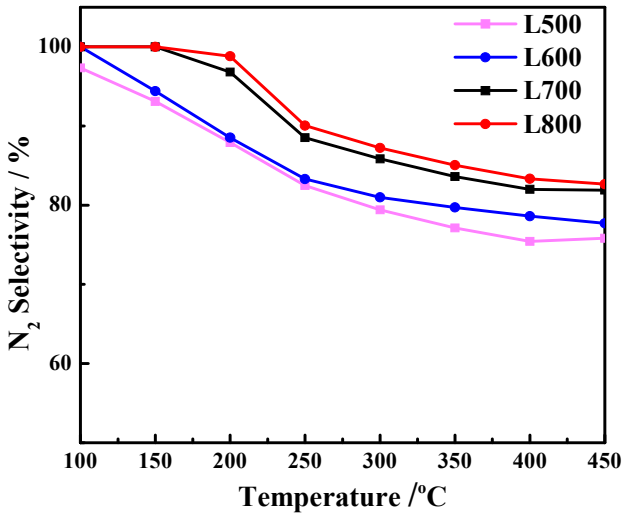

Fig. 3. N_2 selectivity over different iron-manganese oxides catalysts.

300°C. These results indicate that the as-prepared catalyst displays a good performance and N_2 selectivity on SCR of NO by NH_3 and the annealing temperature also significantly affects the performance. The good performance is ascribed to the existence of active component of iron-manganese oxides. The performance of iron-manganese oxides had been documented in previous reports (Kim *et al.*, 2012; Yang *et al.*, 2013; Huang *et al.*, 2014; Huang *et al.*, 2016). Generally, iron oxides possessed a good performance at the temperature of 300–400°C, while manganese oxides exhibited a good performance at the temperature of 150–250°C. Moreover, iron oxides catalyst usually had a better N_2 selectivity than manganese oxides. In this study, the excellent reactivity of high NO conversion and N_2 selectivity in the medium-and-low temperature should ascribe to the presence of iron-manganese oxides. The Fe_2O_3 derived from the decomposition of α-FeOOH is provided with large surface area (Liu *et al.*, 2013b), namely active sites. The existence of manganese oxide also provided active component, which favored the oxidation of NO to NO_2. The existence of NO_2 is beneficial for the fast SCR reaction (Eq. (4)) which is an important process in low-temperature SCR. The fast SCR reaction rate is much quicker than that of standard SCR reaction (Eq. (5)) (Yang *et al.*, 2011; Colombo *et al.*, 2012; Yang *et al.*, 2013; Mihai *et al.*, 2014). It indicates that the SCR reactivity of the as-prepared iron-manganese oxides is considerably dependent on the surface area and pore structure.

On the other hand, as well known, Eqs. (6) and (7) are the common side reactions during the SCR. The increasing reaction temperature promoted the reaction of Eqs. (6) and (7). Combined with the results of NO and NH_3 conversion, it can be concluded that NH_3 was oxidized to NO and N_2O during the reaction temperature over 300°C. In addition, as shown in Fig. 2, the relatively low annealing temperature favored the NO conversion. Therefore, the N_2 selectivity decreases with the increase of reaction temperature and annealing temperature.

$$NO + NO_2 + 2NH_3 \rightarrow 2N_2 + 3H_2O \quad (4)$$

$$4NO + 4NH_3 + O_2 \rightarrow 4N_2 + 6H_2O \quad (5)$$

$$4NH_3 + 5O_2 \rightarrow 4NO + 6H_2O \quad (6)$$

$$2NH_3 + 2O_2 \rightarrow N_2O + 3H_2O \quad (7)$$

XRD and XRF

To make the active component clear, XRD was utilized to characterize the phase composition of the catalyst. The XRD patterns of catalysts are shown in Fig. 4. A weak reflection at 2θ = 36.7° is found and identified as goethite. The weak reflection is intimately related with the crystallinity of goethite. These reflections at 2θ = 20.9°, 26.7°, 50.2° and 2θ = 24.2°, 33.2°, 35.7° can be observed and identified as quartz (SiO_2) and hematite (α-Fe_2O_3), respectively. The intensity of hematite reflections increases with increasing anneal temperature, which contributes to the growth of hematite crystal. In detail, the particle sizes of L500, L600, L700 and L800 for (104) plane are 19.3, 23.7, 27.4, and 33.6 nm, which were obtained by the software of MDI Jade. Obviously, the increasing annealing temperature increases the size of α-Fe_2O_3, which reduces the active sites and results in the decrease of SCR performance. Besides, the results of XRF shows the limonite is composed of Fe_2O_3 (67.18 wt%), MnO (19.68 wt%) and SiO_2 (6.68 wt%). The iron oxide (Fe_2O_3) is identified by XRD pattern, however the manganese oxide is not found. One possible reason is the high dispersion of manganese oxides with very small size. Anyway, the existence of α-Fe_2O_3 and manganese oxides is proved by the XRD and XRF results, respectively. Meanwhile, the annealing temperature significantly influences the crystal size and consequently affects the SCR performance.

SEM and TEM of Raw Material

The SEM, TEM images and corresponding EDS of natural limonite are displayed in Fig. 5. Many lumps composed of a large number of short rod-like presenting a size of nano-scale are observed in the SEM image. Likewise, the rod-like substances with a size of about 10–30 nm are existent in TEM image. Besides, some acicular substances and aggregations with a low contrast are also found. Combining with EDS results and aforementioned XRD results, it can be concluded that the rod-like substance should be goethite, and manganese oxides accrete with goethite. The aggregation with a low contrast should be some clays which can be considered as a carrier to disperse iron and manganese oxides.

As discussed above, the natural limonite is composed of goethite, quartz, manganese oxides, and some clays. The thermal transformation of goethite generates hematite which played an important role in SCR of NO by NH_3. The presence of manganese oxides considerably increased the low-temperature SCR activity of the samples, due to enhanced oxidation of NO to NO_2.

Specific Surface Area and Pore Structure

To characterize the variation of pore structure in more detail, the surface area, pore volume, average pore size as

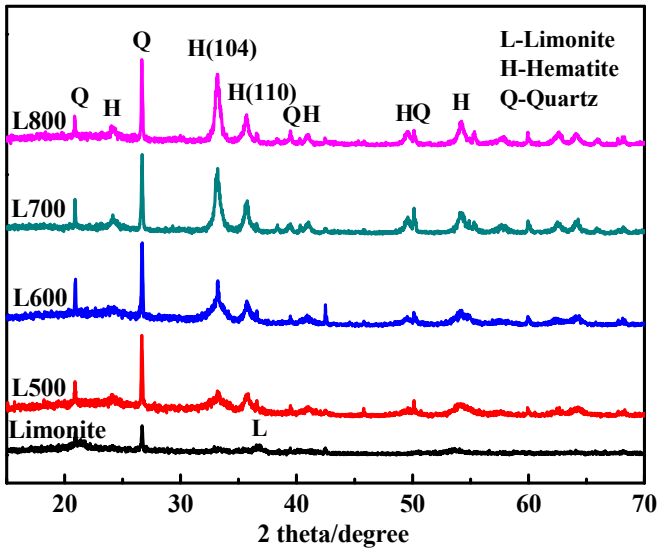

Fig. 4. XRD patterns of different iron-manganese oxides catalysts.

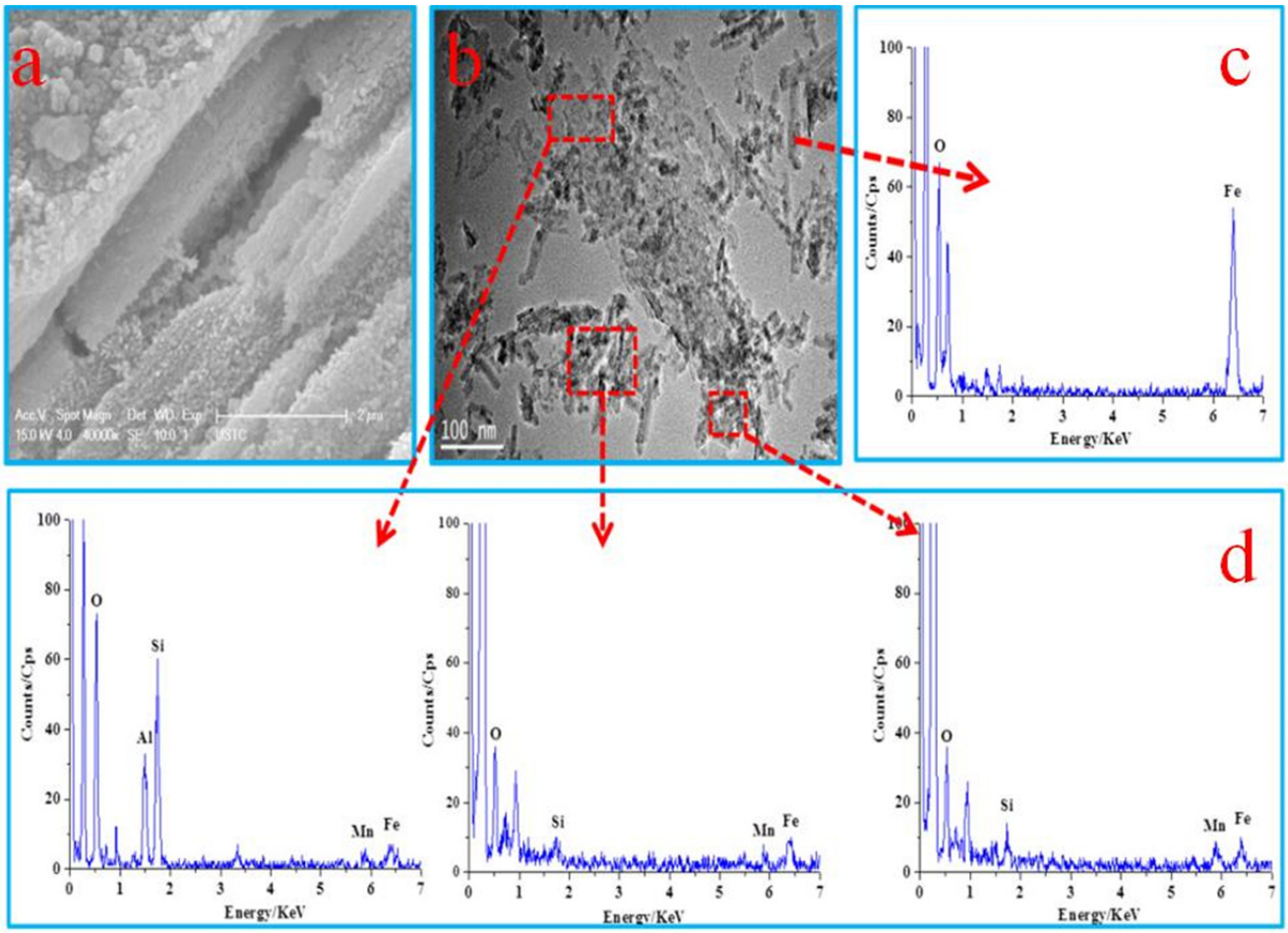

Fig. 5. The SEM (a), TEM (b) images and EDS spectrum (c, d) of natural limonite.

well as the pore distribution were characterized by a pore size and surface area analyzer. The N_2 adsorption-desorption curves of four samples are shown in Fig. 6. It is clearly observed that all the curves of isotherms are similar and close to the type IV, namely porous property. Moreover, the hysteresis loop, at a high relative pressure, decreased with the increasing thermal treatment temperature, indicating the decrease of surface area. The as-prepared iron and manganese

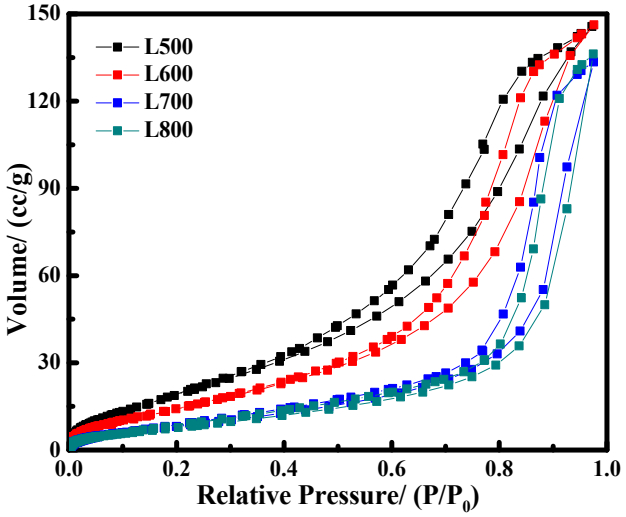

Fig. 6. N_2 adsorption-desorption curves of different iron and manganese oxides catalysts.

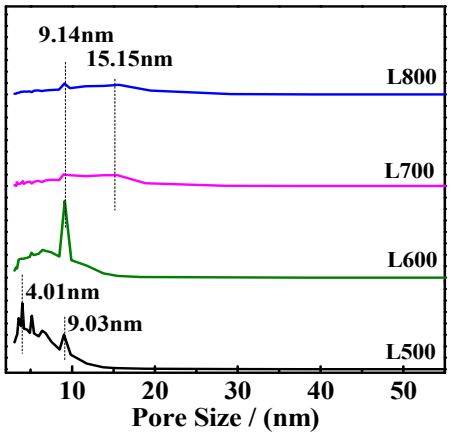

Fig. 7. Pore distribution of different iron and manganese oxides catalysts.

oxides embodied the microporous and mesoporous properties deduced from results of N_2 adsorption-desorption curves, especially for L500 catalyst. The textural properties are also presented by the data of specific surface area, pore volume, and average pore size. As presented in Table 1, the surface area experiences an obvious decrease from 83.27 to 31.68 m^2 g^{-1} as the annealing temperature increases from 500 to 800°C, and meanwhile the average pore size increases from 10.82 to 36.6 nm. The pore size distribution of samples is presented in Fig. 7. As the annealing temperature is 500°C, the pore size distribution is mainly from 2.8 to 10 nm, consistent with the average pore size of 10.82 nm obtained from the N_2-adsorption-desorption.

As well known, catalysts with a large surface area are propitious to a catalytic reaction due to the more number of active sites. Thereby, excellent NO conversion was observed over L500, L600 catalyst under the experimental conditions. Moreover, the increasing order of SCR activity of the catalyst is as follows: L500 > L600 > L700 > L800. Therefore, it can be concluded that the variation of surface area is at least partly responsible for the fluctuation of SCR performance of the as-prepared catalysts.

XPS

The surface elements of catalysts were characterized using XPS, and the results are shown in Fig. 8. From the curves of Fe 2p, the binding energies of Fe 2p (711 and 724.5 eV) correspond well to Fe^{3+} (Mihai *et al.*, 2014). Similarly, the binding energies of Mn 2p (653.7 and 642.5 eV) correspond well to Mn^{4+} (Zhang *et al.*, 2015). Combined with the result of XRD and XRF, the Fe element exists as a state of α-Fe_2O_3 and the Mn is mainly in the form of MnO_2. That is why the Mn-rich limonite after annealing exhibits a high SCR performance and N_2 selectivity at the medium-and-low temperature.

NH_3-TPD

The NH_3-TPD profiles of the four samples are shown in Fig. 9. Three NH_3 desorption peaks are clearly observed from 50 to 500°C for all samples. As reported previously (Liu *et al.*, 2011c), the desorption of physisorbed NH_3 and Lewis acid sites adsorbed with NH_3 were found at 54°C and 193°C, respectively, while the desorption of NH_3 bound to strong Brönsted acid sites at a temperature over 350°C was also confirmed (Ayari *et al.*, 2013; Mejri *et al.*, 2016). Consequently, the large broad bands from 120 to 150°C are ascribed to the desorption of physisorbed NH_3. The desorption peaks at about 240°C and 350°C are attributed to Lewis acid sites and Brönsted acid sites, respectively. In particular, it is speculated that NH_4^+ and coordinated NH_3 formed over the prepared catalysts, especially for L500 and L600 catalysts, because NH_4^+ bound to strong Brönsted acid sites and coordinated NH_3 bound to Lewis acid sites, respectively. In view of the quality analysis, in the whole temperature range L500 shows the largest NH_3 adsorption amount. The NH_3 adsorption amounts of L500, L600, L700, L800 are determined as 83700, 74600, 29900, 7600 μmol g^{-1}, respectively. Namely, the decrease of adsorption amount is in the following sequence: L500 > L600 > L700 > L800 which is in line with the NO conversion and surface area data of the four samples. Therefore, it is suggested that low annealing temperature inhibits the growth of active component, increases the surface area and enhances the SCR performance of NO by NH_3.

Table 1. Surface area, pore volume, and average pore size of different iron and manganese oxides.

Sample	BET / m^2 g^{-1}	Total Pore Volume / cc g^{-1}	Average Pore Size / nm
L500	83.27	0.252	10.82
L600	60.90	0.226	14.86
L700	33.71	0.207	24.51
L800	31.68	0.211	36.60

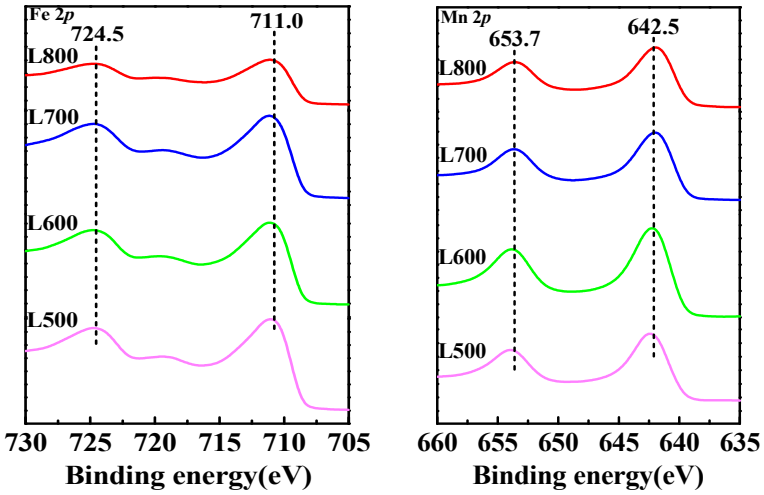

Fig. 8. XPS results of Fe 2*p* and Mn 2*p* of different iron and manganese oxides catalysts.

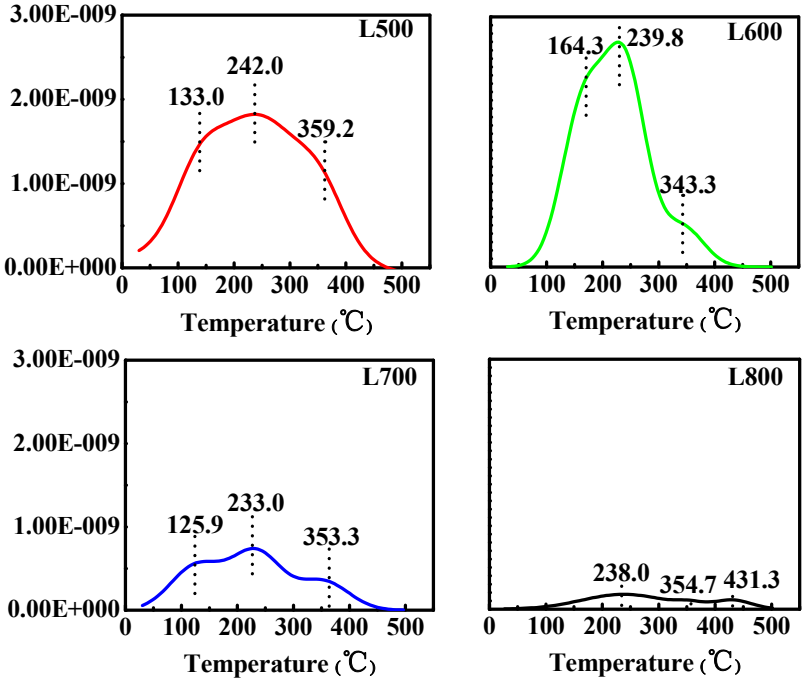

Fig. 9. NH_3-TPD profiles of different iron and manganese oxides catalysts.

Raman

Raman spectroscopy was used to further analysis the crystalline phase and valences of Mn in this study. The Raman spectra of samples are shown in Fig. 10. Previous studies (Bersani *et al.*, 2000; Zoppi *et al.*, 2010) showed that the bands appearing at 220, 290, 403, 500, 609, 650 cm^{-1} were commonly assigned to hematite. However, the band at 650 cm^{-1} is usually a low-intensity signal and the literature (León *et al.*, 2004) reported that it was not the spectrum of a perfect hematite due to the lack of long-range order. On the other hand, earlier work (Buciuman *et al.*, 1999; Hong *et al.*, 2011) confirmed that the Raman spectrum of the MnO_2 appear in the range of 580–650 cm^{-1}. Thereby, the band at 650 cm^{-1} is ascribed to MnO_2. This result is well in agreement with the previous XPS results. The XPS and Raman results proved the existence of MnO_2 in the annealed products, which determined the excellent SCR performance of iron and manganese oxides.

CONCLUSION

Iron and manganese oxides with a nano size were obtained by annealing of natural limonite, a kind of naturally occurred and abundant reserved mineral material. The annealing temperature significantly influenced the surface physicochemical properties and resulted in the fluctuation of SCR performance. The particle size increases from 19.3 to 33.6 nm, and meanwhile the surface area decreased from 83.27 to 31.68 nm as the temperature increased from 500 to 800°C. Besides, the NH_3 adsorption amount also experienced

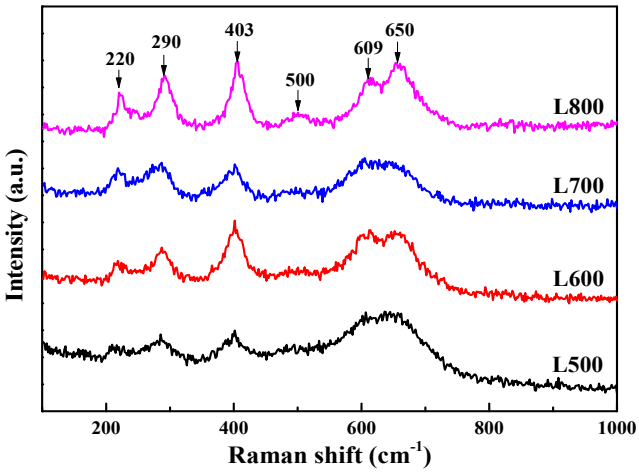

Fig. 10. Raman spectra of different iron and manganese oxides catalysts.

an evident decrease from 83700 to 7600 μmol g^{-1}. The coexistence of iron and manganese oxides, larger surface area and strong surface activity enhanced the SCR reactivity of NO by NH_3 over L500 catalyst. In this present study, the as-prepared iron and manganese oxides exhibited an excellent performance in NO conversion and N_2 selectivity, and are proved to be an effective material as SCR catalyst. The results will provide a novel preparation method for the eco-friendly, low-cost and high-effective SCR catalyst and explore a new approach for the potential application of natural limonite. In addition, based on the experimental results, the investigation on resistance to SO_2 poisoning, lifetime, and synergetic efficiency between α-Fe_2O_3 and MnO_2 will be carried out in future work.

ACKNOWLEDGEMENT

This study was financially supported by the Anhui Provincial Natural Science Foundation (1708085MD87), the China Postdoctoral Science Foundation funded project (No. 2014MM551794), the Fundamental Research Funds for the Central Universities (No. 2014HGCH0007, JZ2017HGTB0196), and the National Natural Science Foundation of China (No. 41572029, 41402030, 41372045, 41772038).

REFERENCES

Ayari, F., Mhamdi, M., Álvarez-Rodríguez, J., Guerrero Ruiz, A.R., Delahay, G. and Ghorbel, A. (2013). Cr–ZSM-5 catalysts for ethylene ammoxidation: Effects of precursor nature and Cr/Al molar ratio on the physicochemical and catalytic properties. *Microporous Mesoporous Mater.* 171: 166–178.

Baksh, M.S., Kikkinides, E.S. and Yang, R.T. (1992). Characterization by physisorption of a new class of microporous adsorbents: Pillared clays. *Ind. Eng. Chem. Res.* 31: 1107–1112.

Bersani, D., Lottici, P.P. and Montenero, A. (2000). A micro-Raman study of iron-titanium oxides obtained by sol-gel synthesis. *J. Mater. Sci.* 35: 4301–4305.

Buciuman, F., Patcas, F., Craciun, R. and Zahn, D.R.T. (1999). Vibrational spectroscopy of bulk and supported manganese oxides. *Phys. Chem. Chem. Phys.* 1: 185–190.

Chen, J.P., Hausladen, M.C. and Yang, R.T. (1995). Delaminated Fe_2O_3-pillared clay: Its preparation, characterization, and activities for selective catalytic reduction of NO by NH_3. *J. Catal.* 151: 135–146.

Colombo, M., Nova, I., Tronconi, E., Schmeißer, V., Bandl-Konrad, B. and Zimmermann, L. (2012). $NO/NO_2/N_2O$–NH_3 SCR reactions over a commercial Fe-Zeolite catalyst for diesel exhaust aftertreatment: Intrinsic kinetics and monolith converter modelling. *Appl. Catal. B* 111: 106–118.

Eigenmann, F., Maciejewski, M. and Baiker, A. (2006). Selective reduction of NO by NH_3 over manganese–cerium mixed oxides: Relation between adsorption, redox and catalytic behavior. *Appl. Catal. B* 62: 311–318.

Fang, D., He, F., Mei, D., Zhang, Z., Xie, J. and Hu, H. (2014). Thermodynamic calculation for the activity and mechanism of Mn/TiO_2 catalyst doped transition metals for SCR at low temperature. *Catal. Commun.* 52: 45–48.

Hong, W.J., Iwamoto, S., Hosokawa, S., Wada, K., Kanai, H. and Inoue, M. (2011). Effect of Mn content on physical properties of CeO_x–MnO_y support and BaO–CeO_x–MnO_y catalysts for direct NO decomposition. *J. Catal.* 277: 208–216.

Huang, H., Lan, Y., Shan, W., Qi, F., Xiong, S., Liao, Y., Fu, Y. and Yang, S. (2014). Effect of sulfation on the selective catalytic reduction of NO with NH_3 over γ-Fe_2O_3. *Catal. Lett.* 144: 578–584.

Huang, L., Wang, X., Yao, S., Jiang, B., Chen, X. and Wang, X. (2016). Cu–Mn bimetal ion-exchanged SAPO-34 as an active SCR catalyst for removal of NO_x from diesel engine exhausts. *Catal. Commun.* 81: 54–57.

Jiang, Y., Wang, X., Xing, Z., Bao, C. and Liang, G. (2017). Preparation and characterization of CeO_2-MoO_3/TiO_2 catalysts for selective catalytic reduction of NO with NH_3. *Aerosol Air Qual. Res., in Press.*

Kapteijn, F., Singoredjo, L., Andreini, A. and Moulijn, J.A. (1994). Activity and selectivity of pure manganese oxides in the selective catalytic reduction of nitric oxide with ammonia. *Appl. Catal. B* 3: 173–189.

Kato, A., Matsuda, S., Nakajima, F., Imanari, M. and Watanabe, Y. (1981). Reduction of nitric oxide with ammonia on iron oxide-titanium oxide catalyst. *J. Phys. Chem.* 85: 1710–1713.

Kim, Y.J., Kwon, H.J., Heo, I., Nam, I.S., Cho, B.K., Jin, W.C., Cha, M.S. and Yeo, G.K. (2012). Mn–Fe/ZSM5 as a low-temperature SCR catalyst to remove NO_x from diesel engine exhaust. *Appl. Catal. B* 126: 9–21.

León, C.P., Kador, L., Zhang, M. and Müller, A.H.E. (2004). In Situ laser-induced formation of α-Fe_2O_3 from Fe^{3+} ions in a cylindrical core-shell polymer brush. *J. Raman Spectrosc.* 35: 165–169.

Liu, C., Yang, S., Ma, L., Peng, Y., Hamidreza, A., Chang, H. and Li, J. (2013a). Comparison on the performance of α-Fe_2O_3 and γ-Fe_2O_3 for selective catalytic reduction of nitrogen oxides with ammonia. *Catal. Lett.* 143: 697–704.

Liu, F. and He, H. (2010). Structure−Activity relationship of iron titanate catalysts in the selective catalytic reduction of NO_x with NH_3. *J. Phys. Chem. C* 114: 16929–16936.

Liu, F., Asakura, K., He, H., Liu, Y., Shan, W., Shi, X. and Zhang, C. (2011a). Influence of calcination temperature on iron titanate catalyst for the selective catalytic reduction of NO_x with NH_3. *Catal. Today* 164: 520–527.

Liu, F., Asakura, K., He, H., Shan, W., Shi, X. and Zhang, C. (2011b). Influence of Sulfation on iron titanate catalyst for the selective catalytic reduction of NO_x with NH_3. *Appl. Catal. B* 103: 369–377.

Liu, F., He, H., Zhang, C., Shan, W. and Shi, X. (2011c). Mechanism of the selective catalytic reduction of NO_x with NH_3 over environmental-friendly iron titanate catalyst. *Catal. Today* 175: 18–25.

Liu, H., Wei, L., Yue, R. and Chen, Y. (2010). CrO_x–CeO_2 binary oxide as a superior catalyst for NO reduction with NH_3 at low temperature in presence of CO. *Catal. Commun.* 11: 829–833.

Liu, H., Chen, T., Qing, C., Xie, Q. and Frost, R.L. (2013b). Confirmation of the assignment of vibrations of goethite: An ATR and IES study of goethite structure. *Spectrochim. Acta, Part A* 116: 154–159.

Liu, H., Chen, T., Zou, X., Qing, C. and Frost, R.L. (2013c). Thermal treatment of natural goethite: Thermal transformation and physical properties. *Thermochim. Acta* 568: 115–121.

Liu, H., Peng, S., Shu, L., Chen, T., Bao, T. and Frost, R.L. (2013d). Magnetic zeolite NaA: Synthesis, characterization based on metakaolin and its application for the removal Cu^{2+}, Pb^{2+}. *Chemosphere* 91: 1539–1546.

Liu, H., Zhang, Z., Li, Q., Chen, T., Zhang, C., Chen, D., Zhu, C. and Jiang, Y. (2017). Novel method for preparing controllable nanoporous α-Fe_2O_3 and its reactivity to SCR De-NO_x. *Aerosol Air Qual. Res.* 17: 1898–1908.

Lu, H.Y., Lin, S.L., Mwangi, J.K., Wang, L.C. and Lin, H.Y. (2016). Characteristics and source apportionment of atmospheric $PM_{2.5}$ at a coastal city in Southern Taiwan. *Aerosol Air Qual. Res.* 16: 1022–1034.

Ma, L., Li, J., Ke, R. and Fu, L. (2011). Catalytic performance, characterization, and mechanism study of $Fe_2(SO_4)_3/TiO_2$ catalyst for selective catalytic reduction of NO_x by ammonia. *J. Phys. Chem. C* 115: 7603–7612.

Mejri, I., Ayari, F., Mhamdi, M., Delahay, G., Ksibi, Z. and Ghorbel, A. (2016). SCR of NO by NH_3 catalyzed by Mo- and V-exchanged zeolite: Effect of Mo precursor salt. *Microporous Mesoporous Mater.* 220: 239–246.

Mihai, O., Widyastuti, C.R., Kumar, A., Li, J., Joshi, S.Y., Kamasamudram, K., Currier, N.W., Yezerets, A. and Olsson, L. (2014). The effect of NO_2/NO_x feed ratio on the NH_3-SCR system over Cu–Zeolites with varying copper loading. *Catal. Lett.* 144: 70–80.

Min, K., Park, E.D., Ji, M.K. and Yie, J.E. (2007). Manganese oxide catalysts for NO_x reduction with NH_3 at low temperatures. *Appl. Catal. A* 327: 261–269.

Mou, X., Zhang, B., Li, Y., Yao, L., Wei, X., Su, D.S. and Shen, W. (2012). Rod-shaped Fe_2O_3 as an efficient catalyst for the selective reduction of nitrogen oxide by ammonia. *Angew. Chem. Int. Ed.* 51: 2989–2993.

Ochońska, J., McClymont, D., Jodłowski, P.J., Knapik, A., Gil, B., Makowski, W., Łasocha, W., Kołodziej, A., Kolaczkowski, S.T. and Łojewska, J. (2012). Copper exchanged ultrastable zeolite Y – A catalyst for NH_3-SCR of NO_x from stationary biogas engines. *Catal. Today* 191: 6–11.

Pérez-RamíRez, J., Kumar, M.S. and Brückner, A. (2004). Reduction of N_2O with CO over FeMFI zeolites: influence of the preparation method on the iron species and catalytic behavior. *J. Catal.* 223: 13–27.

Putluru, S.S.R., Schill, L., Jensen, A.D., Siret, B., Tabaries, F. and Fehrmann, R. (2015). Mn/TiO_2 and Mn–Fe/TiO_2 catalysts synthesized by deposition precipitation—promising for selective catalytic reduction of NO with NH_3 at low temperatures. *Appl. Catal. B* 165: 628–635.

Rattigan, O.V., Civerolo, K.L., Felton, H.D., Schwab, J.J. and Demerjian, K.L. (2016). Long term trends in New York: $PM_{2.5}$ Mass and particle components. *Aerosol Air Qual. Res.* 16: 1191–1205.

Sahu, S.K. (2015). High resolution emission inventory of NO_x and CO for mega city Delhi, India. *Aerosol Air Qual. Res.* 15: 1137–1144.

Schneider, H., Maciejewski, M., Kohler, K., Wokaun, A. and Baiker, A. (1995). Chromia supported on titania: VI. Properties of different chromium oxide phases in the catalytic reduction of NO by NH_3 studied by *in situ* diffuse reflectance FTIR spectroscopy. *J. Catal.* 157: 312–320.

Schuricht, F. and Reschetilowski, W. (2012). Simultaneous selective catalytic reduction (SCR) of NO_x and N_2O over Ag/ZSM-5 – Catalytic studies and mechanistic implications. *Microporous Mesoporous Mater.* 164: 135–144.

Shin, B., Chun, H.H., Cha, J.S., Shin, M.C. and Lee, H. (2016). Physico-chemical property and catalytic activity of a CeO_2-Doped MnO_x-TiO_2 catalyst with SO_2 resistance for low-temperature NH_3-SCR of NO_z. *J. Nanosci. Nanotechnol.* 16: 4370.

Xu, W., Yu, Y., Zhang, C. and He, H. (2008). Selective catalytic reduction of NO by NH_3 over a Ce/TiO_2 catalyst. *Catal. Commun.* 9: 1453–1457.

Yang, S., Wang, C., Li, J., Yan, N., Ma, L. and Chang, H. (2011). Low temperature selective catalytic reduction of NO with NH_3 over Mn–Fe spinel: Performance, mechanism and kinetic study. *Appl. Catal. B* 110: 71–80.

Yang, S., Liu, C., Chang, H., Ma, L., Qu, Z., Yan, N., Wang, C. and Li, J. (2013). Improvement of the activity of γ-Fe_2O_3 for the selective catalytic reduction of NO with NH_3 at high temperatures: NO reduction versus NH_3 oxidization. *Ind. Eng. Chem. Res.* 52: 5601–5610.

Yang, S., Qi, F., Xiong, S., Dang, H., Liao, Y., Wong, P.K. and Li, J. (2016). MnO_x supported on Fe–Ti spinel: A novel Mn based low temperature SCR catalyst with a high N_2 selectivity. *Appl. Catal. B* 181: 570–580.

Yoshida, M., Nobukawa, T., Ito, S.I., Tomishige, K. and Kunimori, K. (2004). Structure sensitivity of ion-exchanged Fe-MFI in the catalytic reduction of nitrous oxide by methane under an excess oxygen atmosphere.

J. Catal. 223: 454–464.

Youn, S., Song, I. and Kim, D.H. (2016). Roles of promoters in V_2O_5/TiO_2 catalysts for selective catalytic reduction of NO_x with NH_3: Effect of order of impregnation. *J. Nanosci. Nanotechnol.* 16: 4350.

Yu, C. (2015). In situ drifts study of the low temperature selective catalytic reduction of NO with NH_3 over MnO_x supported on multi-walled carbon nanotubes catalysts. *Aerosol Air Qual. Res.* 15: 1017–1027.

Yu, X., Cao, F., Zhu, X., Zhu, X., Gao, X., Luo, Z. and Cen, K. (2017). Selective catalytic reduction of NO over Cu-Mn/OMC catalysts: Effect of preparation method. *Aerosol Air Qual. Res.* 17: 302–313.

Zahaf, R. (2015). Pt catalyst over SiO_2 and Al_2O_3 supports synthesized by aerosol method for HC-SCR denox application. *Aerosol Air Qual. Res.* 15: 2409–2421.

Zhang, Y., Zheng, Y., Wang, X. and Lu, X. (2015). Preparation of Mn–FeO_x/CNTs catalysts by redox co-Precipitation and application in low-temperature NO reduction with NH_3. *Catal. Commun.* 62: 57–61.

Zhu, Z., Liu, Z., Liu, S. and Niu, H. (1999). A novel carbon-supported vanadium oxide catalyst for NO reduction with NH_3 at low temperatures. *Appl. Catal. B* 23: L229–L233.

Zoppi, A., Lofrumento, C., Castellucci, E.M. and Migliorini, M.G. (2010). The raman spectrum of hematite: Possible indicator for a compositional or firing distinction among terra sigillata wares. *Anal. Chim.* 95: 239–246.

Received for review, July 11, 2017
Revised, August 18, 2017
Accepted, August 20, 2017